

Resonant tunneling of holes in double-barrier heterostructures in the envelope-function approximation

R. Wessel

*Hochfeld-Magnetlabor, Max-Planck-Institut für Festkörperforschung, Boîte Postale 166X,
F-38042 Grenoble CEDEX, France*

M. Altarelli

*European Synchrotron Radiation Facility, Boîte Postale 220, F-38043 Grenoble CEDEX, France
and Hochfeld-Magnetlabor, Max-Planck-Institut für Festkörperforschung, Boîte Postale 166X,
F-38042 Grenoble CEDEX, France*

(Received 31 October 1988; revised manuscript received 6 February 1989)

A transfer-matrix calculation of the resonant tunneling of holes in double-barrier heterostructures is presented, based on a four-band description of hole subbands. The mixing of heavy- and light-hole channels at nonvanishing in-plane \mathbf{k} vectors produces a variety of line shapes of the transmission coefficient through different resonances, some of which with pronounced asymmetry. Most of these asymmetric line shapes are suppressed by the integration over initial states contributing to the tunneling current between two p -type electrodes. The mixing effects increase with the thickness of the barriers. A discussion of the relevance of these calculations for the interpretation of measurements and for the design of new experiments is presented.

I. INTRODUCTION

Resonant tunneling of electrons through double-barrier heterostructures (DBH) was first investigated by Tsu and Esaki¹ and has extensively been studied experimentally²⁻⁷ and theoretically using the transfer matrix,^{1,8-12} the transfer Hamiltonian formalism,^{13,14} or wave packets.^{15,16} Inelastic processes are included in some models.¹⁷⁻¹⁹

Holes are of interest because of degeneracy at the top of the valence band, which provides the possibility of mixing and tunneling through the structure via different LH and HH channels. Mendez *et al.*²⁰ observed resonant tunneling of holes through GaAs-AlAs DBH and found that the results cannot be described with independent light- and heavy-hole (LH and HH, respectively) states. In this paper we apply an extension of the transfer-matrix technique using a four-band effective-mass equation, for which exact solutions were recently given.²¹ In our model we neglect the spin-orbit split-off band and also inelastic effects.

The paper is organized as follows: in Sec. II we summarize the formalism, recall the functions in the bulk and boundary conditions at potential steps, and present an extension of the transfer-matrix technique to calculate the transmission amplitudes. In Sec. III we discuss results for the transmission coefficient as a function of energy for some typical DBH and for various values of the in-plane wave vector (k_{\parallel}). For nonvanishing k_{\parallel} mixing of LH and HH states occurs. The mixing increases not only with increasing k_{\parallel} but also with increasing barrier width.

Interesting structure in the line shape occurs because of interference of different channels. In Sec. IV we calculate the current and compare the results with experiment.²⁰ Some of the interesting features of the transmission line shapes do not appear in the current, due to integration over initial states up to the Fermi energy. The possibility of experimental configurations displaying interference effects in the line shapes are briefly discussed. Finally, in Sec. V, we summarize the results and conclusions.

II. METHOD OF CALCULATION

The envelope-function approximation^{22,23} for electronic states in semiconductors is derived from the effective-mass Hamiltonian of Luttinger and Kohn²⁴. Neglecting the conduction and spin-orbit bands, the effective-mass Hamiltonian is a 4×4 matrix operator H which acts on a four-component envelope function $\mathbf{F}(\mathbf{r}) = (F_1(\mathbf{r}), F_2(\mathbf{r}), F_3(\mathbf{r}), F_4(\mathbf{r}))$. Solutions for the effective-mass equation in the bulk,

$$H\mathbf{F}(\mathbf{r}) = E\mathbf{F}(\mathbf{r}), \quad (1)$$

were explicitly written by Andreani *et al.*²¹ (see the Appendix) and their notation is adopted in this paper. The total wave function is, approximately,²³

$$\varphi(\mathbf{r}) = \mathbf{F}(\mathbf{r}) \cdot \mathbf{u}_0(\mathbf{r}) = \mathbf{f} e^{i\mathbf{k} \cdot \mathbf{r}} \cdot \mathbf{u}_0(\mathbf{r}), \quad (2)$$

where for a constant potential $\mathbf{F}(\mathbf{r}) = \mathbf{f} e^{i\mathbf{k} \cdot \mathbf{r}}$ and \mathbf{f} is one of the eigenvectors (A4). \mathbf{u}_0 is the periodic part of the Bloch functions,

$$\mathbf{u}_0(\mathbf{r}) = (u_{10}(\mathbf{r}), u_{20}(\mathbf{r}), u_{30}(\mathbf{r}), u_{40}(\mathbf{r})) = (u_{3/2,0}(\mathbf{r}), u_{1/2,0}(\mathbf{r}), u_{-1/2,0}(\mathbf{r}), u_{-3/2,0}(\mathbf{r})).$$

In each region of constant potential $V(z)=\text{const}$ (see Fig. 1), the wave function $\psi(\mathbf{r})$ is a linear combination of bulk solutions for a given E and k_x, k_y with corresponding $k_z = \pm k_l, \pm k_h$.

For example, in region (b) (see Fig. 1),

$$\begin{aligned} \psi^{(b)}(\mathbf{r}) = & [b_1 \mathbf{V}_1^{(b)}(+k_h)e^{ik_h z} + b_2 \mathbf{V}_2^{(b)}(+k_l)e^{ik_l z} + b_3 \mathbf{V}_3^{(b)}(+K_l)e^{ek_l z} + b_4 \mathbf{V}_4^{(b)}(+k_h)e^{ik_h z} \\ & + b_5 \mathbf{V}_1^{(b)}(-k_h)e^{-k_h z} + b_6 \mathbf{V}_2^{(b)}(-k_l)e^{-ik_l z} + b_7 \mathbf{V}_3^{(b)}(-k_l)e^{-ik_l z} + b_8 \mathbf{V}_4^{(b)}(-k_h)e^{-ik_h z}] \cdot \mathbf{u}_0(\mathbf{r}) e^{i(k_x x + k_y y)} \\ \equiv & \phi^{(b)}(z) \cdot \mathbf{u}_0(\mathbf{r}) e^{i(k_x x + k_y y)}. \end{aligned} \quad (3)$$

k_z is derived from (A3) where E is replaced by $E - V_0^{(b)}$.

For large k_{\parallel} and small E , it can happen that either k_l alone or both k_l and k_h become imaginary in the GaAs regions. In this case only bulk solutions that vanish at infinity must be taken into account in the electrodes. For given incoming amplitudes a_j ($j=1,2,3,4$), the amplitudes b_j are fixed by the boundary conditions at each interface z_m .

In the approximation that the periodic part of the Bloch function $\mathbf{u}_0(\mathbf{r})$ are equal in both layers and with the assumption that k_x and k_y are conserved during tunneling, the boundary conditions are²³

$$\phi(z) \text{ continuous at } z_m, \quad (4)$$

$$\underline{B}\phi(z) \text{ continuous at } z_m.$$

The matrix \underline{B} [given in (A6)] is derived by integrating the effective-mass equation across an interface.²³ Using

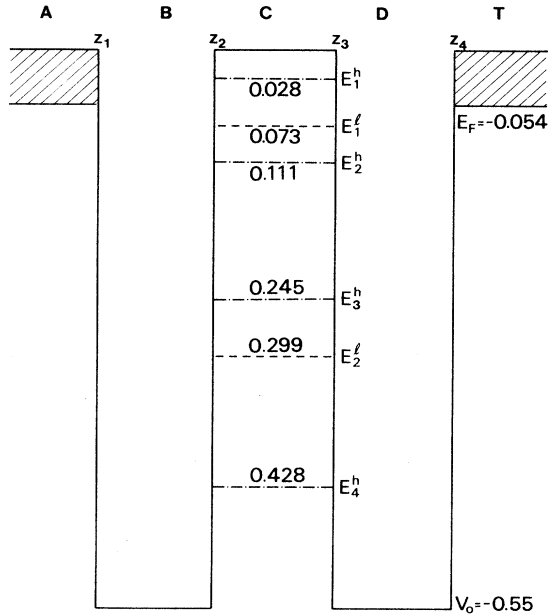


FIG. 1. Typical potential structure for resonant hole tunneling experiments. The potential depth $V_0 = -0.55$ eV and the well width $w_{\text{well}} = 50$ Å are used throughout this paper. The barrier width w_{barrier} will be varied. The resonance energies (eV) of a structure with $w_{\text{barrier}} = 10$ Å are indicated [$k_x = k_y = 0.0016(2\pi/a)$, lattice constant $a = 5.65$ Å].

the transfer-matrix technique,^{1,8-12} but now for the four-component function $\phi(z)$, we get from (3), (4), and (A6) at each interface an equation for the amplitudes. For example, at $z = z_2$,

$$\underline{M}_3 \mathbf{b} = \underline{M}_4 \mathbf{c}, \quad (5)$$

where \underline{M}_3 is a complex 8×8 matrix which contains the coefficients of b_i in (3). The amplitudes \mathbf{c} are a function of the amplitudes \mathbf{b} ,

$$\mathbf{c} = (\underline{M}_4)^{-1} \underline{M}_3 \mathbf{b}. \quad (6)$$

Analogous equations at each interface give the transmission amplitudes \mathbf{t} as a function of the incoming amplitudes \mathbf{a} :

$$\mathbf{t} = (\underline{M}_8)^{-1} \underline{M}_7 (\underline{M}_6)^{-1} \underline{M}_5 (\underline{M}_4)^{-1} \underline{M}_3 (\underline{M}_2)^{-1} \underline{M}_1 \mathbf{a}. \quad (7)$$

The transfer matrix \underline{M} is defined with use of (7),

$$\begin{pmatrix} t_1 \\ t_2 \\ t_3 \\ t_4 \\ 0 \\ 0 \\ 0 \\ 0 \end{pmatrix} = \underline{M} \begin{pmatrix} a_1 \\ a_2 \\ a_3 \\ a_4 \\ r_1 \\ r_2 \\ r_3 \\ r_4 \end{pmatrix}. \quad (8)$$

The lower part of (8) gives the reflection amplitudes r_j as a function of the incoming amplitudes a_j . The transmission amplitudes t_n are then calculated by the upper part of (8).

The transmission coefficient D_n through channel n is, for example, in the case of an incoming HH state ($a_1 = 1$, $a_2 = a_3 = a_4 = 0$),

$$D_n = \frac{\langle \phi_n^{(t)} | j_z | \phi_n^{(t)} \rangle}{\langle \phi_1^{(a)} | j_z | \phi_1^{(a)} \rangle} = |t_n|^2 N, \quad (9)$$

where N is a normalization factor and the probability current-density operator is given in Ref. 25.

III. TRANSMISSION COEFFICIENT

In Fig. 2 we show the transmission coefficients D_n for an incoming HH state [means $a_1 = 1$, $a_2 = a_3 = a_4 = 0$ in (8)] through the different HH and LH channels [D_1, D_2, D_3 in (9) correspond to states with $m_j = +\frac{3}{2}, +\frac{1}{2}, -\frac{1}{2}$]. Since D_4 ($m_j = -\frac{3}{2}$) is about 10 orders of magnitude smaller, it is not shown.

The incoming HH state is strongly mixed into LH states. The mixing appears as a peak for transmission into the HH channel D_1 [Fig. 2(a)] at the resonance energy corresponding to a quasistationary LH state in the quantum well. Also, HH resonances occur in the LH channels [Figs. 2(b), and 2(c)]. Strong asymmetric line

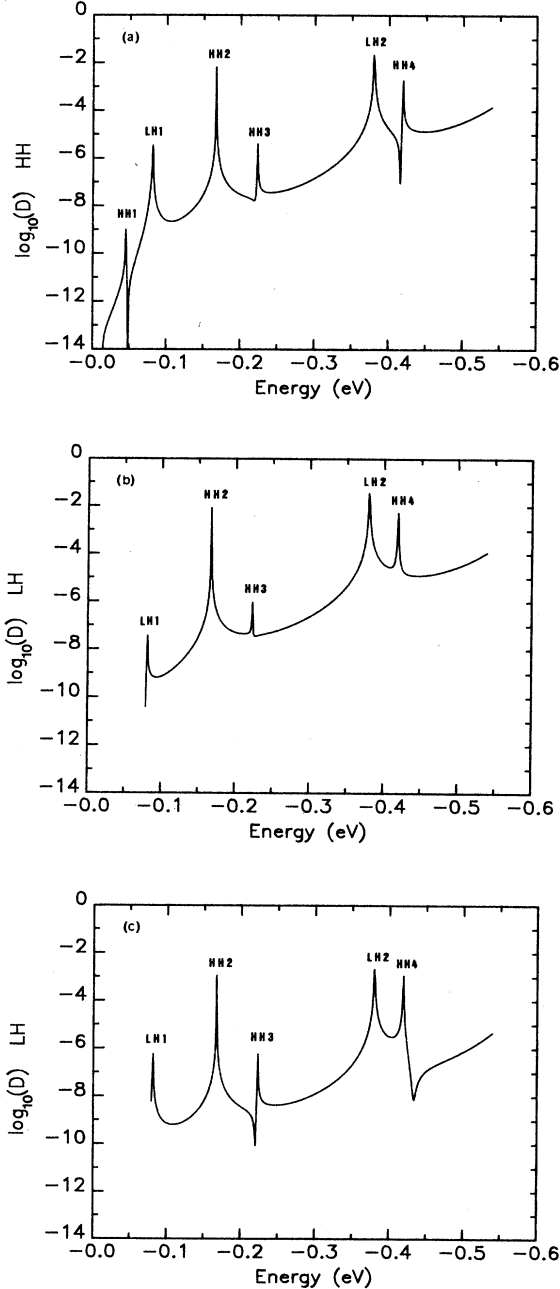


FIG. 2. Transmission coefficient of an incoming HH state ($a_1=1$) through a DBH with $V_0=-0.55$ eV, $w_{\text{well}}=50$ Å, $w_{\text{barrier}}=30$ Å, $k_x=k_y=0.036(2\pi/a)$ (lattice constant $a=5.65$ Å). (a) Outgoing HH channel ($m_j=+\frac{3}{2}$); (b) outgoing LH channel ($m_j=+\frac{1}{2}$); and (c) outgoing LH channel ($m_j=-\frac{1}{2}$).

shapes occur because of interference of resonant HH amplitudes with off-resonant LH amplitudes.

For different k_x and k_y , mixing effects change drastically since the off-diagonal elements in (A1) are linear or quadratic functions of k_x and k_y . For the calculation of the current in Sec. IV, it is important to notice that a larger k_{\parallel} produces average transmission coefficients D_n which are larger by several orders of magnitude. The shift in the energy position of the resonance peaks with k_{\parallel} reflects the in-plane band structure $E(k_{\parallel})$ of the quantum well.²⁶

For this value of k_{\parallel} , k_l as calculated from (A3) is imaginary in the GaAs regions for $|E|$ smaller than 80 meV. Only *decaying* light-hole bulk solutions contribute to the wave function in the electrodes. Therefore, the flux through the LH channels is 0 and, from (9), $D_{2,3}=0$ for $|E|$ smaller than 80 meV.

Results for barriers thinner by a factor of 3 show that the mixing is drastically reduced in comparison with Fig. 2. The increase in mixing with increasing barrier width can be understood as an increase in mixing with increasing lifetime of the quasibound state in the quantum well.

Calculations for the incoming LH state show that in the outgoing LH channel the average transmission coefficient is several orders of magnitude larger. In this case the peaks at HH resonance energies are not as prominent as the peaks at LH resonance energies for the incoming HH state in the outgoing HH channel. Due to time-reversal symmetry the transmission coefficient for incoming HH state in the outgoing LH channel and for the incoming LH state in the outgoing HH channel are equal.

IV. CURRENT

The current density through DBH between two p^+ -type electrodes is²⁷

$$j = \sum_{l=1}^4 \frac{e}{(2\pi)^2 \hbar} \int_{E_F}^{\min\{E_F+eU, 0\}} dE \int_{k_{\parallel}(0)}^{k_{\parallel}(E)} dk_{\parallel} k_{\parallel} \times D_l(E, k_{\parallel}, V, U), \quad (10)$$

where the sum goes over all incoming HH and LH states ($m_j = \pm\frac{3}{2}, \pm\frac{1}{2}$).

In the calculation of D the potential (Fig. 1) with bias is approximated by three regions of constant potential where the electrostatic potential is averaged over each region. The result for a typical structure as in Fig. 1 is shown in Fig. 3.

In the k -space regions identified by $|E| \leq |E_F|$, heavy-hole states have real k_z values up to k_{\parallel} values much larger than for light holes. Furthermore, the transmission coefficients D_n increase with k_{\parallel} by several orders of magnitude and nonvanishing k_{\parallel} causes strong mixing. As a result, most of the current comes from incoming HH states, even at the LH resonances.

Mendez *et al.*²⁰ see structure in the conductance of the resonant hole tunneling DBH. In Table I we compare these results with the bias values at the current peaks in

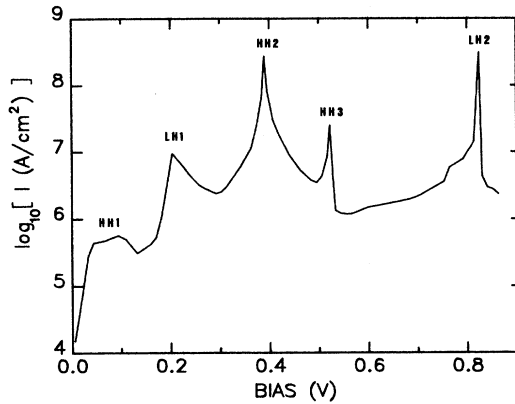


FIG. 3. Tunnel current of holes through a DBH. The structure parameters are $w_{\text{barrier}} = 10 \text{ \AA}$, $w_{\text{well}} = 50 \text{ \AA}$, $V_0 = -0.55 \text{ eV}$, $E_F = -0.055 \text{ eV}$ (compare Fig. 1). The figure shows the sum of incoming HH and LH states and the sum of all outgoing channels. As discussed in the text, the current comes mostly from incoming HH states.

Fig. 3. For numerical reasons in the calculation 10-\AA barriers were used instead of 50-\AA barriers in the experiment. In this approximation, we ignore the lifetime effect mentioned above and the effect of the barrier width on the in-plane band structure $E(k_{\parallel})$ ²⁶

Mendez and co-workers²⁰ did not mention the doping of the electrodes, so the Fermi energy in our calculations is just an estimate. The last two experimental values are not calculated because the above-mentioned approximation for the potential in presence of bias is bad at high bias. When considering Table I, one should keep in mind the three approximations ($10\text{-}50\text{-\AA}$ barriers, estimate of E_F , step approximation for the potential) mentioned above. Calculated resonance voltages are brought into agreement with experimental values by multiplying with a fitted factor 1.76. This factor accounts for voltage drops outside the double-barrier region, which are mentioned in Ref. 20.

It is interesting to consider whether different experimental configurations may be adopted, to observe the interference effects which we described before, but which are not observable in tunneling current measurements of the type of Ref. 20. To this aim, it would be desirable to select the heavy or light character of the holes in the in-

coming and outgoing channels. If a photoconductive experiment is performed, electron-hole pairs with prescribed heavy- or light-hole character can be generated with polarized light.^{28,29} On the other hand, the selection of the outgoing channel may exploit the different drift velocities of heavy and light holes, towards the collection electrode, in a time-resolved experiment. A possibility is, in principle, presented by a reverse-biased $p^+ - i - n^+$ diode,³⁰ where a double AIAs barrier is adjacent to the p^+ -type region and the photogenerated holes are created in a wide intrinsic GaAs layer between the second barrier and the n^+ -type electrode. Bias can be adjusted so that electrons are immediately swept to the n^+ -type electrode and do not tunnel through the barriers, while holes are removed only via the much slower tunneling process through the double barrier.

V. SUMMARY AND CONCLUSION

We have presented an extension of the transfer-matrix technique using the four-component envelope functions. The formalism is applied to calculate the transmission coefficient and the tunnel current of holes through DBH. Strong mixing occurs between LH and HH states. The mixing increases not only with increasing in-plane k vector, but also with the lifetime of the quasibound state in the well. The latter effect corresponds to an increasing of mixing with the barrier width. The transmission of HH states through light-hole resonances is much stronger than the other way around. This may suppress the observation of HH resonances in the experiment if the HH resonance energy is close to a LH resonance energy. The mixing provides the interference of resonance amplitudes with off-resonance amplitudes, which produce several interesting (strongly asymmetric) line shapes.

The tunnel current is calculated and an estimate to compare with experiment is done. Due to integration over initial states up to the Fermi energy, the above mentioned line shapes are hidden.

Some suggestion for experimental configurations which might give the possibility to show part of the line shapes is discussed.

ACKNOWLEDGMENTS

We are grateful to Dr. L. C. Andreani for very useful discussions on the current operator for holes. Numerical

TABLE I. Comparison of measured (Ref. 20) resonances in the current, with bias of the current peaks in Fig. 3 (taking into account a factor 1.76 for voltage drops in the electrodes, see text).

	HH1	LH1	HH2	HH3	LH2		
Voltage at which structure occurs in the experiment (Ref. 20)	0.2	0.43	0.67	1.15	1.45	1.81	2.33
Voltage at which current peaks in Fig. 3 times 1.76	0.14	0.37	0.69	0.92	1.44		

calculations were performed with resources made available by the Centre de Calcul Vectoriel pur la Recherche, Palaiseau, France.

APPENDIX

Basic equations from Andreani *et al.*²¹ are used in this paper. The effective-mass Hamiltonian in the four-band approximation is

$$H = - \begin{pmatrix} P+Q & L & M & 0 \\ L^\dagger & P-Q & 0 & M \\ M^\dagger & 0 & P-Q & -L \\ 0 & M^\dagger & -L^\dagger & P+Q \end{pmatrix} + V, \quad (\text{A1})$$

where

$$\begin{aligned} P &= \frac{\gamma_1}{2m_0} k^2, \\ L &= \frac{-i\sqrt{3}\gamma_3}{m_0} (k_x - ik_y)k_z, \\ Q &= \frac{\gamma_2}{2m_0} (k_x^2 + k_y^2 - 2k_z^2), \\ M &= \frac{\gamma_2\sqrt{3}}{2m_0} (k_x^2 - k_y^2) - i\frac{\gamma_3\sqrt{3}}{m_0} k_x k_y. \end{aligned} \quad (\text{A2})$$

The eigenvalues are

$$E = -P \pm (Q^2 + LL^\dagger + MM^\dagger)^{1/2}. \quad (\text{A3})$$

The plus sign refers to HH states and the minus sign to Lh states.

The eigenvectors are

$$\begin{aligned} \mathbf{V}_1 &= \begin{pmatrix} R_1 \\ L^\dagger \\ M^\dagger \\ 0 \end{pmatrix}, \quad \mathbf{V}_2 = \begin{pmatrix} -L \\ R_2 \\ 0 \\ -M^\dagger \end{pmatrix}, \\ \mathbf{V}_3 &= \begin{pmatrix} -M \\ 0 \\ R_2 \\ L^\dagger \end{pmatrix}, \quad \mathbf{V}_4 = \begin{pmatrix} 0 \\ M \\ -L \\ R_1 \end{pmatrix}, \end{aligned} \quad (\text{A4})$$

where

$$R_1 = Q - P - E, \quad R_2 = Q + P + E. \quad (\text{A5})$$

For $k_x = k_y = 0$, $\mathbf{V}_1, \mathbf{V}_4$ are the HH eigenvectors and $\mathbf{V}_2, \mathbf{V}_3$ are the LH eigenvectors.

The boundary condition matrix is

$$\underline{B} = \begin{pmatrix} (\gamma_1 - 2\gamma_2)(\partial/\partial z) & \sqrt{3}\gamma_3(k_x - ik_y) & 0 & 0 \\ -\sqrt{3}\gamma_3(k_x + ik_y) & (\gamma_1 + 2\gamma_2)(\partial/\partial z) & 0 & 0 \\ 0 & 0 & (\gamma_1 + 2\gamma_2)(\partial/\partial z) & -\sqrt{3}\gamma_3(k_x - ik_y) \\ 0 & 0 & \sqrt{3}\gamma_3(k_x + ik_y) & (\gamma_1 - 2\gamma_2)(\partial/\partial z) \end{pmatrix}. \quad (\text{A6})$$

¹R. Tsu and L. Esaki, Appl. Phys. Lett. **22**, 562 (1973).

²L. L. Chang, L. Esaki, and R. Tsu, Appl. Phys. Lett. **24**, 593 (1974).

³V. J. Goldmann, D. C. Tsui, and J. E. Cunningham, Phys. Rev. Lett. **58**, 1256 (1987).

⁴T. C. L. G. Sollner, W. D. Goodhue, P. E. Tannenwald, C. D. Parker, and D. D. Peck, Appl. Phys. Lett. **43**, 588 (1983).

⁵M. A. Reed, J. W. Lee, and H. L. Tsai, Appl. Phys. Lett. **49**, 158 (1986).

⁶J. Söderström, T. G. Anderson, and J. Westin, Superlatt. Microstruct. **3**, 283 (1987).

⁷H. Morkoç, J. Chen, U. K. Reddy, T. Henderson, and S. Luryi, Appl. Phys. Lett. **49**, 70 (1986).

⁸E. O. Kane, in *Tunneling Phenomena in Solids*, edited by E. Burstein and S. Lundqvist (Plenum, New York, 1969), Chap. 1.

⁹M. O. Vassel, J. Lee, and H. F. Lockwood, J. Appl. Phys. **54**, 5206 (1983).

¹⁰L. A. Cury and N. Studart, Superlatt. Microstruct. **3**, 175 (1987).

¹¹L. A. Cury and N. Studart (unpublished).

¹²B. Ricco and M. Ya. Azbel, Phys. Rev. B **29**, 1970 (1984).

¹³M. C. Payne, J. Phys. C **19**, 1145 (1986).

¹⁴T. Weil and B. Vinter, Appl. Phys. Lett. **50**, 1281 (1987).

¹⁵K. W. H. Stevens, J. Phys. C **17**, 5735 (1984).

¹⁶A. P. Jauho and M. M. Nieto, Superlatt. Microstruct. **2**, 407 (1986).

¹⁷S. Luryi, Appl. Phys. Lett. **47**, 491 (1985).

¹⁸A. Douglas Stone and P. A. Lee, Phys. Rev. Lett. **54**, 1196 (1985).

¹⁹M. Büttiger, IBM J. Res. Dev. **32**, 63 (1988).

²⁰E. E. Mendez, W. I. Wang, B. Ricco, and L. Esaki, Appl. Phys. Lett. **47**, 415 (1985).

²¹L. C. Andreani, A. Pasquarello, and F. Bassani, Phys. Rev. B **36**, 5887 (1987).

²²G. Bastard and J. A. Brum, IEEE J. Quantum Electron. **QE-22**, 1625 (1986).

²³M. Altarelli, in *Proceedings of Les Houches Winter School, Semiconductors, Superlattices and Heterojunctions*, edited by G. Allan, G. Bastard, N. Boccarda, M. Lunnou, and M. Voos (Springer, New York, 1986).

²⁴J. M. Luttinger and W. Kohn, Phys. Rev. **97**, 869 (1955).

- ²⁵M. Altarelli, in *Semiconductor Physics*, Vol. 177 of *Lecture Notes in Physics*, edited by G. Landwehr (Springer, Berlin, 1983).
- ²⁶R. Wessel and M. Altarelli, *Phys. Rev. B* **39**, 10 246 (1989).
- ²⁷C. B. Duke, *Tunneling in Solids* (Academic, New York, 1969).
- ²⁸R. Sooryakumar, D. S. Chemla, A. Pinczuk, A. Gossard, W. Wiegmann, and L. J. Sham, *J. Vac. Sci. Technol. B* **2**, 349 (1984).
- ²⁹R. Sauer, K. Thonke, and W. T. Sang, *Phys. Rev. Lett.* **61**, 609 (1988).
- ³⁰R. T. Collins, K. v. Klitzing, and K. Ploog, *Phys. Rev. B* **33**, 4378 (1986).